QUARTERLY OF APPLIED MATHEMATICS
VOLUME LVIII, NUMBER 1
MARCH 2000, PAGES 17–36

CONSERVATIVE MOTION OF A DISCRETE, TETRAHEDRAL TOP ON A SMOOTH HORIZONTAL PLANE

BY

DONALD GREENSPAN

Abstract. Tetrahedral tops are simulated as discrete, rigid bodies in rotation by introducing a molecular mechanics formulation. The contact point of the top with the (X, Y)-plane is allowed to move in the plane. The conservative, dynamical differential equations are solved numerically in such a fashion that all the system invariants are preserved. Examples, which include cusp formation, and looping, are described and discussed.

1. Introduction. Rigid body motion is of fundamental interest in mathematics, science, and engineering. In this paper we will introduce a new, simplistic approach to this area of study in the spirit of modern molecular mechanics. We will consider a discrete, tetrahedral body and simulate its motion when it spins like a top whose contact point with the (X, Y)-plane is allowed to move in the plane. The approach will not require the use of special coordinates, Cayley-Klein parameters, tensors, dyadics, or related concepts [1]. All that will be required is Newtonian mechanics in three-dimensional (X, Y, Z)-space. The numerical methodology will conserve exactly the same energy, linear momentum, and angular momentum as does the associated differential system. Computer examples, run in double precision on a 64-bit Alpha 275 personal computer, which exhibit precession, nutation, cusp formation, and looping, will be described and discussed.

2. A discrete, rigid tetrahedral top. Consider, as shown in Fig. 2.1, a regular tetrahedron with vertices $P_i(x_i, y_i, z_i)$, $i = 1, 2, 3, 4$, and edge length R. For convenience set

$$(x_1, y_1, z_1) = (0, 0, R\sqrt{6}/3), \qquad (x_2, y_2, z_2) = (0, R\sqrt{3}/3, 0),$$
$$(x_3, y_3, z_3) = (\tfrac{1}{2}R, -R\sqrt{3}/6, 0), \qquad (x_4, y_4, z_4) = (-\tfrac{1}{2}R, -R\sqrt{3}/6, 0).$$

The geometric center of triangle $P_2P_3P_4$ is $(0, 0, 0)$ and the geometric center of the tetrahedron is $(0, 0, R\sqrt{6}/12)$.

Received October 3, 1996.
2000 *Mathematics Subject Classification.* Primary 37M05, 65L12, 70F25.

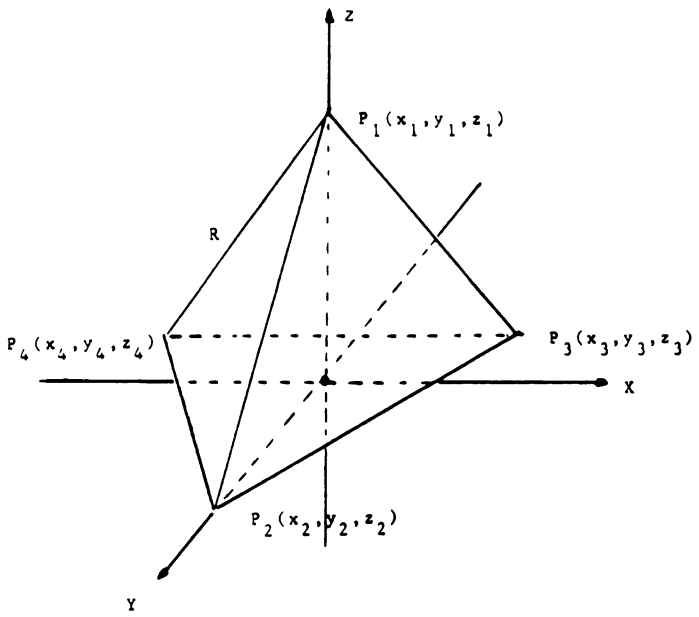

FIG. 2.1

In order to create a top, let us first invert the tetrahedron in Fig. 2.1 to the position shown in Fig. 2.2, so that

$$(x_1, y_1, z_1) = (0, 0, 0), \qquad (x_2, y_2, z_2) = (0, R\sqrt{3}/3, R\sqrt{6}/3),$$
$$(x_3, y_3, z_3) = (\tfrac{1}{2}R, -R\sqrt{3}/6, R\sqrt{6}/3), \qquad (x_4, y_4, z_4) = (-\tfrac{1}{2}R, -R\sqrt{3}/6, R\sqrt{6}/3).$$

The geometric center of triangle $P_2P_3P_4$ is now $(0, 0, R\sqrt{6}/3)$, while the geometric center $\overline{P} = (\overline{x}, \overline{y}, \overline{z})$ of the inverted tetrahedron is $(0, 0, R\sqrt{6}/4)$.

Next, let us set P_2, P_3, P_4 in rotation in the plane $z = R\sqrt{6}/3$. As shown in Fig. 2.3, we let the velocity of each particle be perpendicular to the line joining that particle to the center of triangle $P_2P_3P_4$. Let P_2, P_3, P_4 each have the same speed V. Thus, we take the velocities $\mathbf{v}_i = (v_{ix}, v_{iy}, v_{iz})$, $i = 1, 2, 3, 4$, of P_1, P_2, P_3, P_4 to be

$$\mathbf{v}_1 = (0, 0, 0), \quad \mathbf{v}_2 = (V, 0, 0), \quad \mathbf{v}_3 = (-\tfrac{1}{2}V, -V\sqrt{3}/2, 0), \quad \mathbf{v}_4 = (-\tfrac{1}{2}V, V\sqrt{3}/2, 0).$$

Finally, we want the rotating tetrahedron to be tilted, initially, relative to the Z-axis, so that we assume the line joining P_1 to $\overline{P}$ forms an angle α relative to the Z-axis. As shown in Fig. 2.4, this will be done by rotating the (X, Z)-plane through an angle α. Thus the new positions (x_i', y_i', z_i') and the new velocities $(v_{ix'}, v_{iy'}, v_{iz'})$, $i = 1, 2, 3, 4$, satisfy

$$x_i' = x_i \cos\alpha + z_i \sin\alpha, \quad y_i' = y_i, \quad z_i' = -x_i \sin\alpha + z_i \cos\alpha,$$
$$v_{ix'} = v_{ix} \cos\alpha + v_{iz} \sin\alpha, \quad v_{iy'} = v_{iy}, \quad v_{iz'} = -v_{ix} \sin\alpha + v_{iz} \cos\alpha.$$

Thus, once the parameters R, V, and α are given, all initial data for a tilted, rotating tetrahedron are determined.

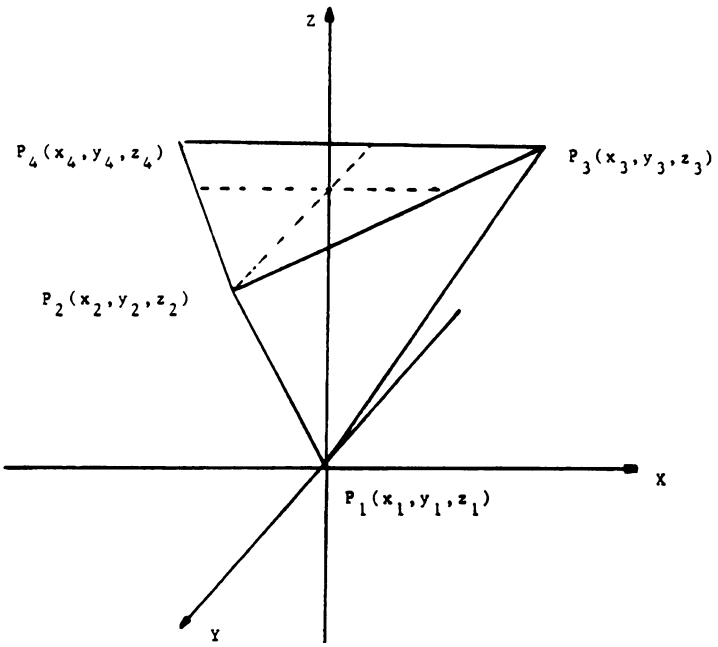

FIG. 2.2

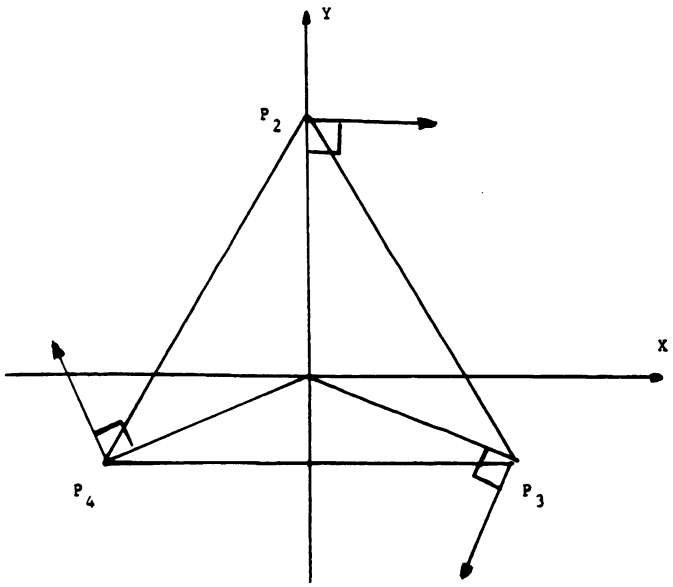

FIG. 2.3

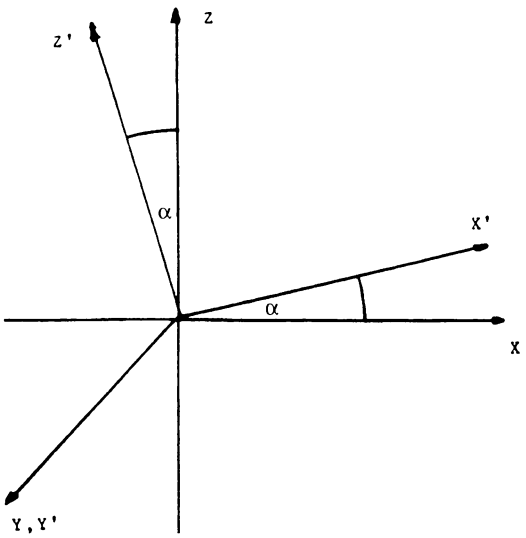

FIG. 2.4

3. Dynamical equations. The motion of our rotating top is now treated as a four-body problem. At any time t, let P_i, $i = 1, 2, 3, 4$, be located at $\mathbf{r} = (x_i, y_i, z_i)$, have velocity $\mathbf{v}_i = (\dot{x}_i, \dot{y}_i, \dot{z}_i) = (v_{ix}, v_{iy}, v_{iz})$, and have acceleration $\mathbf{a}_i = (\ddot{x}_i, \ddot{y}_i, \ddot{z}_i) = (\dot{v}_{ix}, \dot{v}_{iy}, \dot{v}_{iz})$. Let the mass of each P_i be m_i. For $i \neq j$, let $\mathbf{r}_{ij}$ be the vector from P_i to P_j and let r_{ij} be the magnitude of $\mathbf{r}_{ij}$, $i = 1, 2, 3, 4$; $j = 1, 2, 3, 4$; $i \neq j$. Let $\phi = \phi(r_{ij})$ be a potential function defined by the pair P_i, P_j, $i \neq j$.

Then, for $i = 1, 2, 3, 4$, the Newtonian dynamical equations for the motion of the particles are the second-order differential equations

$$m_i a_{ix} = -\frac{\partial \phi}{\partial r_{ij}} \frac{x_i - x_j}{r_{ij}} - \frac{\partial \phi}{\partial r_{ik}} \frac{x_i - x_k}{r_{ik}} - \frac{\partial \phi}{\partial r_{im}} \frac{x_i - x_m}{r_{im}}, \tag{3.1}$$

$$m_i a_{iy} = -\frac{\partial \phi}{\partial r_{ij}} \frac{y_i - y_j}{r_{ij}} - \frac{\partial \phi}{\partial r_{ik}} \frac{y_i - y_k}{r_{ik}} - \frac{\partial \phi}{\partial r_{im}} \frac{y_i - y_m}{r_{im}}, \tag{3.2}$$

$$m_i a_{iz} = -\frac{\partial \phi}{\partial r_{ij}} \frac{z_i - z_j}{r_{ij}} - \frac{\partial \phi}{\partial r_{ik}} \frac{z_i - z_k}{r_{ik}} - \frac{\partial \phi}{\partial r_{im}} \frac{z_i - z_m}{r_{im}} - g_i. \tag{3.3}$$

In (3.1)–(3.3), $i = 1$ implies $j = 2, k = 3, m = 4$; $i = 2$ implies $j = 1, k = 3, m = 4$; $i = 3$ implies $j = 1, k = 2, m = 4$; $i = 4$ implies $j = 1, k = 2, m = 3$. Moreover, we choose $g_1 = 0, g_2 = g_3 = g_4 > 0$, so that gravity acts only on P_2, P_3, and P_4.

The equations (3.1)–(3.3) are fully conservative, that is, they conserve system energy, linear momentum, and angular momentum [1], [2], which are called the system invariants.

4. Numerical method. In order to solve system (3.1)–(3.3) in a fashion that conserves exactly the same energy, linear momentum, and angular momentum, we first

rewrite (3.1)–(3.3) as the following equivalent first-order system:

$$\frac{dx_i}{dt} = v_{ix}, \tag{4.1}$$

$$\frac{dy_i}{dt} = v_{iy}, \tag{4.2}$$

$$\frac{dz_i}{dt} = v_{iz}, \tag{4.3}$$

$$m_i \frac{dv_{ix}}{dt} = -\frac{\partial \phi}{\partial r_{ij}} \frac{x_i - x_j}{r_{ij}} - \frac{\partial \phi}{\partial r_{ik}} \frac{x_i - x_k}{r_{ik}} - \frac{\partial \phi}{\partial r_{im}} \frac{x_i - x_m}{r_{im}}, \tag{4.4}$$

$$m_i \frac{dv_{iy}}{dt} = -\frac{\partial \phi}{\partial r_{ij}} \frac{y_i - y_j}{r_{ij}} - \frac{\partial \phi}{\partial r_{ik}} \frac{y_i - y_k}{r_{ik}} - \frac{\partial \phi}{\partial r_{im}} \frac{y_i - y_m}{r_{im}}, \tag{4.5}$$

$$m_i \frac{dv_{iz}}{dt} = -\frac{\partial \phi}{\partial r_{ij}} \frac{z_i - z_j}{r_{ij}} - \frac{\partial \phi}{\partial r_{ik}} \frac{z_i - z_k}{r_{ik}} - \frac{\partial \phi}{\partial r_{im}} \frac{z_i - z_m}{r_{im}} - g_i. \tag{4.6}$$

We now choose difference equation approximations for (4.1)–(4.6). For a fixed time step Δt, let $t_n = n\Delta t$, $n = 0, 1, 2, 3, \ldots$. At t_n let P_i be at $\mathbf{r}_{i,n} = (x_{i,n}, y_{i,n}, z_{i,n})$ with velocity $\mathbf{v}_{i,n} = (v_{i,x,n}, v_{i,y,n}, v_{i,z,n})$. Then (4.1)–(4.6) will be approximated by

$$\frac{x_{i,n+1} - x_{i,n}}{\Delta t} = \frac{v_{i,x,n+1} + v_{i,x,n}}{2}, \tag{4.7}$$

$$\frac{y_{i,n+1} - y_{i,n}}{\Delta t} = \frac{v_{i,y,n+1} + v_{i,y,n}}{2}, \tag{4.8}$$

$$\frac{z_{i,n+1} - z_{i,n}}{\Delta t} = \frac{v_{i,z,n+1} + v_{i,z,n}}{2}, \tag{4.9}$$

$$\begin{aligned} m_i \frac{v_{i,x,n+1} - v_{i,x,n}}{\Delta t} = &-\frac{\phi(r_{ij,n+1}) - \phi(r_{ij,n})}{r_{ij,n+1} - r_{ij,n}} \cdot \frac{x_{i,n+1} + x_{i,n} - x_{j,n+1} - x_{j,n}}{r_{ij,n+1} + r_{ij,n}} \\ &- \frac{\phi(r_{ik,n+1}) - \phi(r_{ik,n})}{r_{ik,n+1} - r_{ik,n}} \cdot \frac{x_{i,n+1} + x_{i,n} - x_{k,n+1} - x_{k,n}}{r_{ik,n+1} + r_{ik,n}} \\ &- \frac{\phi(r_{im,n+1}) - \phi(r_{im,n})}{r_{im,n+1} - r_{im,n}} \cdot \frac{x_{i,n+1} + x_{i,n} - x_{m,n+1} - x_{m,n}}{r_{im,n+1} + r_{im,n}}, \end{aligned} \tag{4.10}$$

$$\begin{aligned} m_i \frac{v_{i,y,n+1} - v_{i,y,n}}{\Delta t} = &-\frac{\phi(r_{ij,n+1}) - \phi(r_{ij,n})}{r_{ij,n+1} - r_{ij,n}} \cdot \frac{y_{i,n+1} + y_{i,n} - y_{j,n+1} - y_{j,n}}{r_{ij,n+1} + r_{ij,n}} \\ &- \frac{\phi(r_{ik,n+1}) - \phi(r_{ik,n})}{r_{ik,n+1} - r_{ik,n}} \cdot \frac{y_{i,n+1} + y_{i,n} - y_{k,n+1} - y_{k,n}}{r_{ik,n+1} + r_{ik,n}} \\ &- \frac{\phi(r_{im,n+1}) - \phi(r_{im,n})}{r_{im,n+1} - r_{im,n}} \cdot \frac{y_{i,n+1} + y_{i,n} - y_{m,n+1} - y_{m,n}}{r_{im,n+1} + r_{im,n}}, \end{aligned} \tag{4.11}$$

$$\begin{aligned} m_i \frac{v_{i,z,n+1} - v_{i,z,n}}{\Delta t} = &-\frac{\phi(r_{ij,n+1}) - \phi(r_{ij,n})}{r_{ij,n+1} - r_{ij,n}} \cdot \frac{z_{i,n+1} + z_{i,n} - z_{j,n+1} - z_{j,n}}{r_{ij,n+1} + r_{ij,n}} \\ &- \frac{\phi(r_{ik,n+1}) - \phi(r_{ik,n})}{r_{ik,n+1} - r_{ik,n}} \cdot \frac{z_{i,n+1} + z_{i,n} - z_{k,n+1} - z_{k,n}}{r_{ik,n+1} + r_{ik,n}} \\ &- \frac{\phi(r_{im,n+1}) - \phi(r_{im,n})}{r_{im,n+1} - r_{im,n}} \cdot \frac{z_{i,n+1} + z_{i,n} - z_{m,n+1} - z_{m,n}}{r_{im,n+1} + r_{im,n}} \\ &- g_i. \end{aligned} \tag{4.12}$$

Difference equations (4.7)–(4.12) are consistent with differential equations (4.1)–(4.6) and conserve exactly the same system invariants [3], [4] as do (3.1)–(3.3). System (4.7)–(4.12), for each of $n = 0, 1, 2, \ldots$, consists of 24 equations in the unknowns $x_{i,n+1}, y_{i,n+1}, z_{i,n+1}, v_{i,x,n+1}, v_{i,y,n+1}, v_{i,z,n+1}$, $i = 1, 2, 3, 4$; and in the knowns $x_{i,n}, y_{i,n}, z_{i,n}, v_{i,x,n}, v_{i,y,n}, v_{i,z,n}$. These are solved readily by Newton's method [3].

Typical FORTRAN programs for generating initial data and for determining resulting trajectories from given initial data are available for the interested reader in the Appendices of Greenspan [5].

5. Examples. In considering examples, we must first choose a potential function ϕ. We do this in cgs units and in such a fashion that we ensure that the tetrahedron is rigid. To accomplish this, we introduce the following classical, molecular-type function [2], [6]:

$$\phi = A\left[-\frac{1}{r_{ij}^3} + \frac{1}{r_{ij}^5}\right], \quad A > 0, \tag{5.1}$$

in which A is sufficiently large to impose rigidity. The choice of exponents in (5.1) prevents the explosive behavior characteristic of real molecules, yet allows for attractive and repulsive interaction, as is desirable for aggregates of molecules [6].

From (5.1), it follows that the magnitude F of the force $\mathbf{F}$ determined by ϕ satisfies

$$F = A\left[-\frac{3}{r_{ij}^4} + \frac{5}{r_{ij}^6}\right].$$

Thus, $F(\bar{r}) = 0$ provided $\bar{r} = (5/3)^{1/2} \sim 1.290994449$.

We now choose the tetrahedral edge length R to be

$$R = 1.290994449. \tag{5.2}$$

For this value of R, the force between any two of the particles is zero, so that the tetrahedron is physically stable. In the examples to be described, the parameters A, g, and m_i are scaled for computational convenience to be $A = 10^6, g = 0.980, m_i = 1$, $i = 1, 2, 3, 4$, unless otherwise specified.

The time step Δt is chosen to be $\Delta t = 10^{-5}$. The positions of P_1 and $\overline{P}$ are recorded every 5000 time steps through 11,000,000 time steps. Thus, 2200 points are available for each trajectory to be described. In the figures to be given, units on the axes are often rescaled to accentuate the character of the resulting trajectory. In all the examples, the distance between any of P_1, P_2, P_3, P_4 is always 1.291. If at any time any one of z_2, z_3, z_4 is zero, the calculations are stopped and it is concluded that the top has fallen and ceased its motion.

To assure that the motion of P_1 is in the (X, Y)-plane, we assume throughout that $v_{1,z,n} = 0$, $n = 0, 1, 2, 3 \ldots$.

EXAMPLE 1. Set $V = 4, \alpha = 15°$. Figure 5.1 shows the cusped path of P_1 in the (X, Y)-plane using the first 350 points of its trajectory and yields just over one complete cycle. There are 6^+ cycles in the 2200 point trajectory shown in Figure 5.2. The point $\overline{P}$ for the entire 2200 point trajectory oscillates on the line $(0.2046144211, 0, z)$, with $\bar{z}$ rising

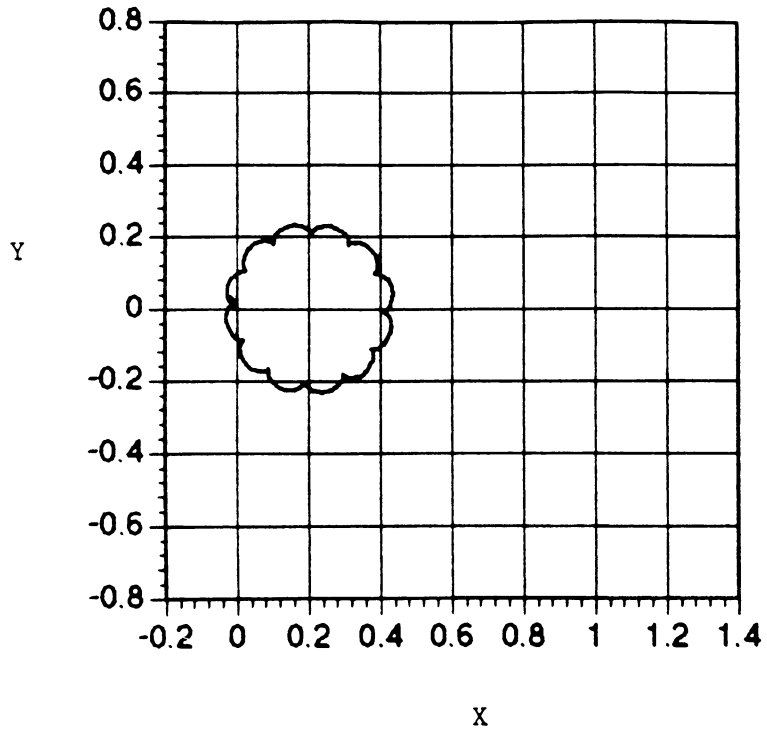

FIG. 5.1

and falling in the range $0.754 < \overline{z} < 0.764$. Thus, the center point of the trajectories shown in Figures 5.1 and 5.2 in the (X, Y)-plane is $(0.2046144211, 0)$.

EXAMPLE 2. Set $V = 8, \alpha = 15°$. Figure 5.3 shows the cusped trajectory of P_1 in the (X, Y)-plane using the first 750 points of its trajectory to yield just over one complete cycle. There are 3^+ cycles in the 2200 point graph shown in Figure 5.4. The point $\overline{P}$ for the entire 2200 point trajectory lies on the line $(0.2046144211, 0, z)$, that is, the same line as in Example 1, but with $\overline{z}$ rising and falling in the range $0.762 < \overline{z} < 0.764$. Thus, the center point of the trajectories shown in Figures 5.3 and 5.4 in the (X, Y)-plane is $(0.2446144211, 0)$. Note that there are more cusps in Figure 5.3 than in Figure 5.1, but these are smaller, and that the trajectory is becoming more circular.

EXAMPLE 3. Set $V = 16, \alpha = 15°$. Figure 5.5 shows a relatively circular trajectory for P_1 in the (X, Y)-plane using all 2200 points, which yield just over 1 cycle. The point $\overline{P}$ for the entire trajectory lies on the line $(0.2046144211, 0, z)$ with $\overline{z}$ in the range $0.763 < \overline{z} < 0.764$.

EXAMPLE 4. Set $V = 4, \alpha = 30°$. Figure 5.6 shows the cusped path of P_1 in the (X, Y)-plane using the first 350 points of its trajectory, which yields just over 1 complete cycle. There are 6^+ cycles in the 2200 point trajectory shown in Figure 5.7. The point $\overline{P}$ for the entire 2200 point trajectory lies on the line $(0.3952847076, 0, z)$, with $\overline{z}$ rising and falling in the range $0.652 < \overline{z} < 0.685$.

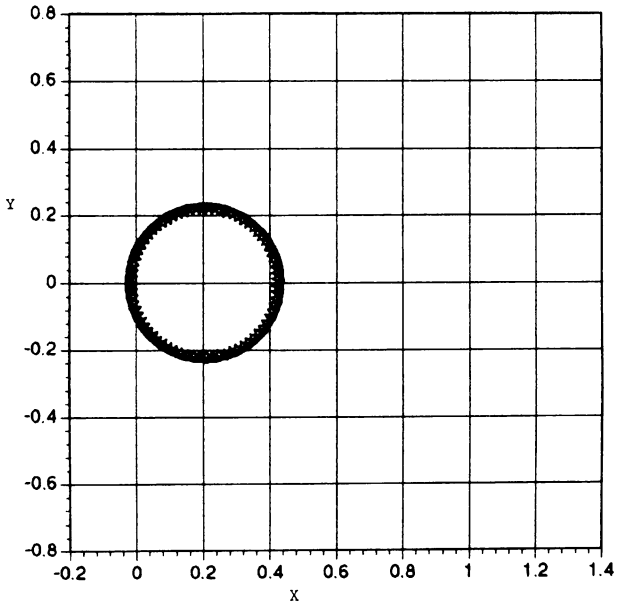
0.8
0.6
0.4
Y 0.2
0
-0.2
-0.4
-0.6
-0.8
-0.2 0 0.2 0.4 0.6 0.8 1 1.2 1.4
X

FIG. 5.2

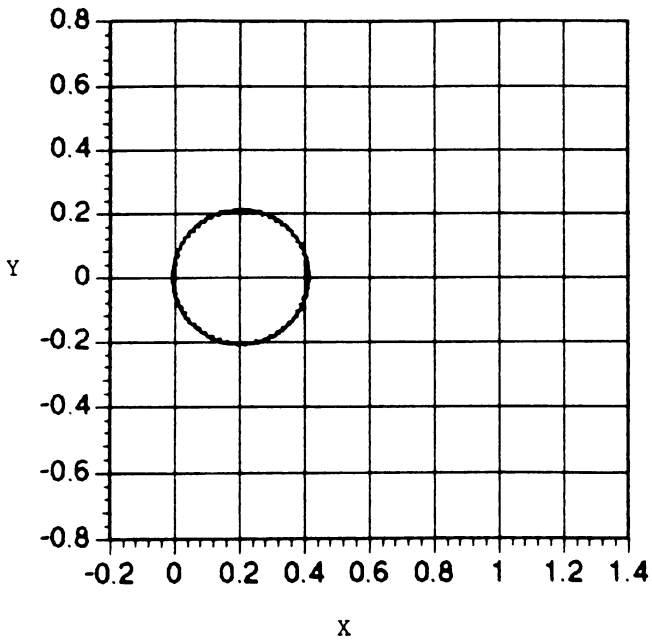
0.8
0.6
0.4
0.2
Y 0
-0.2
-0.4
-0.6
-0.8
-0.2 0 0.2 0.4 0.6 0.8 1 1.2 1.4
X

FIG. 5.3

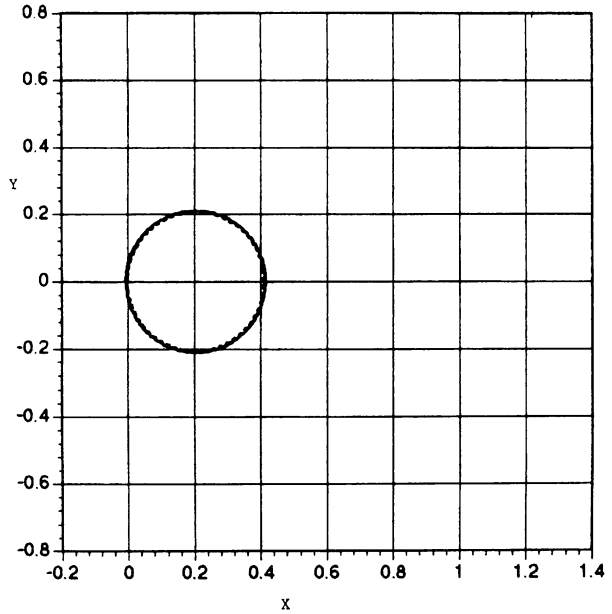
0.8
0.6
0.4
Y
0.2
0
-0.2
-0.4
-0.6
-0.8
-0.2
0
0.2
0.4
0.6
0.8
1
1.2
1.4
X

FIG. 5.4

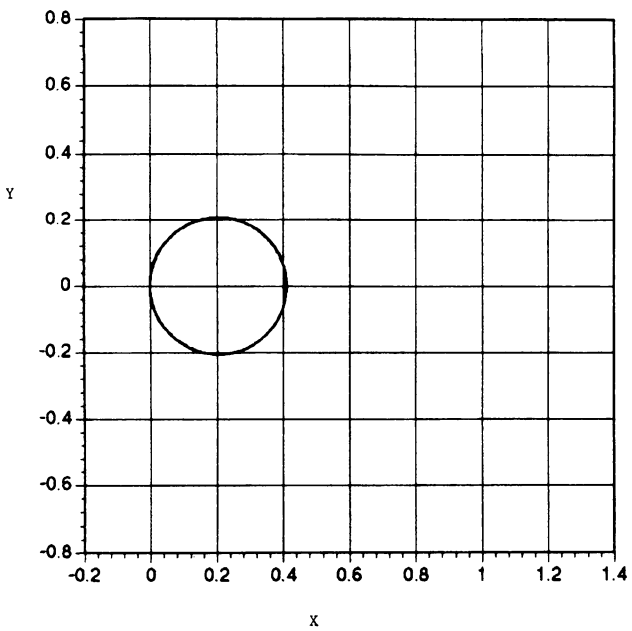
0.8
0.6
0.4
Y
0.2
0
-0.2
-0.4
-0.6
-0.8
-0.2
0
0.2
0.4
0.6
0.8
1
1.2
1.4
X

FIG. 5.5

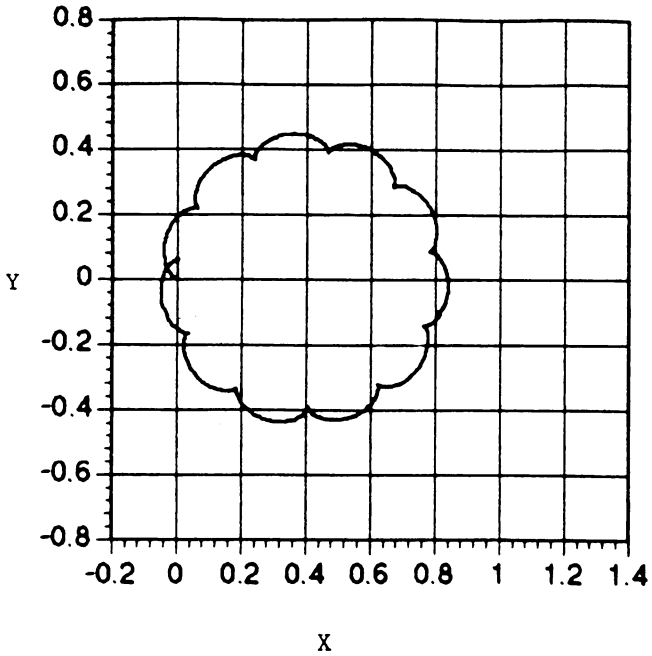
0.8
0.6
0.4
0.2
Y 0
-0.2
-0.4
-0.6
-0.8
-0.2 0 0.2 0.4 0.6 0.8 1 1.2 1.4
X

FIG. 5.6

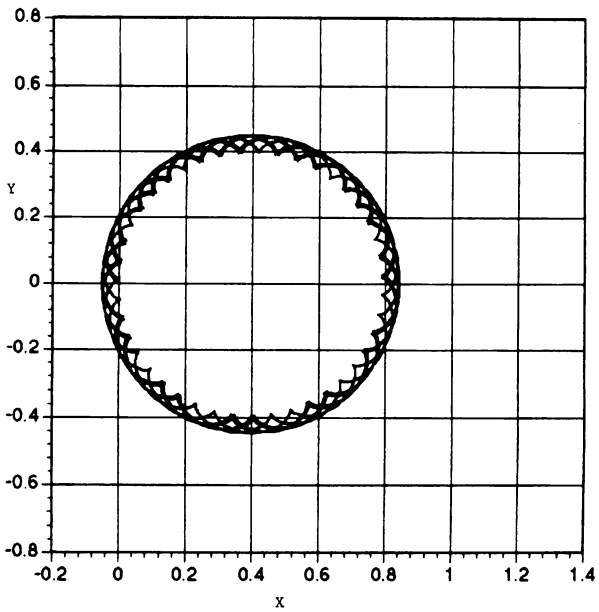
0.8
0.6
0.4
Y
0.2
0
-0.2
-0.4
-0.6
-0.8
-0.2 0 0.2 0.4 0.6 0.8 1 1.2 1.4
X

FIG. 5.7

EXAMPLE 5. Set $V = 8, \alpha = 30°$. Figure 5.8 shows the cusped path of P_1 in the (X, Y)-plane for the first 750 points of its trajectory, which yields just over 1 complete cycle. There are 3^+ cycles in the entire 2200 point trajectory shown in Figure 5.9. The point $\overline{P}$ for the entire 2200 point trajectory lies on the line $(0.3952847076, 0, z)$, with $\overline{z}$ rising and falling in the range $0.678 < \overline{z} < 0.685$. Compared to Example 4, the number of cusps is increasing but their size is decreasing.

EXAMPLE 6. Set $V = 16, \alpha = 30°$. Figure 5.10 shows a relatively circular path for P_1 using all 2200 trajectory points, which yield just over 1 cycle. The center of the circle is $(0.3952847076, 0)$. The point $\overline{P}$ is always on the line $(0.3952847076, 0, z)$, with $\overline{z}$ in the range $0.683 < \overline{z} < 0.685$.

EXAMPLE 7. Set $V = 4, \alpha = 45°$. Figure 5.11 shows the cusped path of P_1 in the (X, Y)-plane using the first 350 points of its trajectory, which yields just over 1 complete cycle. There are 6^+ cycles in the 2200 point trajectory shown in Figure 5.12. The point $\overline{P}$ always lies on the line $(0.5590169945, 0, z)$, with $\overline{z}$ rising and falling in the range $0.497 < \overline{z} < 0.559$.

EXAMPLE 8. Set $V = 8, \alpha = 45°$. Figure 5.13 shows the cusped path of P_1 in the (X, Y)-plane for the first 750 points of its trajectory, which yields just over 1 complete cycle. There are 3^+ cycles in the entire 2200 point trajectory shown in Figure 5.14. The point $\overline{P}$ is always on the line $(0.5590169945, 0, z)$, with $\overline{z}$ rising and falling in the range $0.545 < \overline{z} < 0.559$.

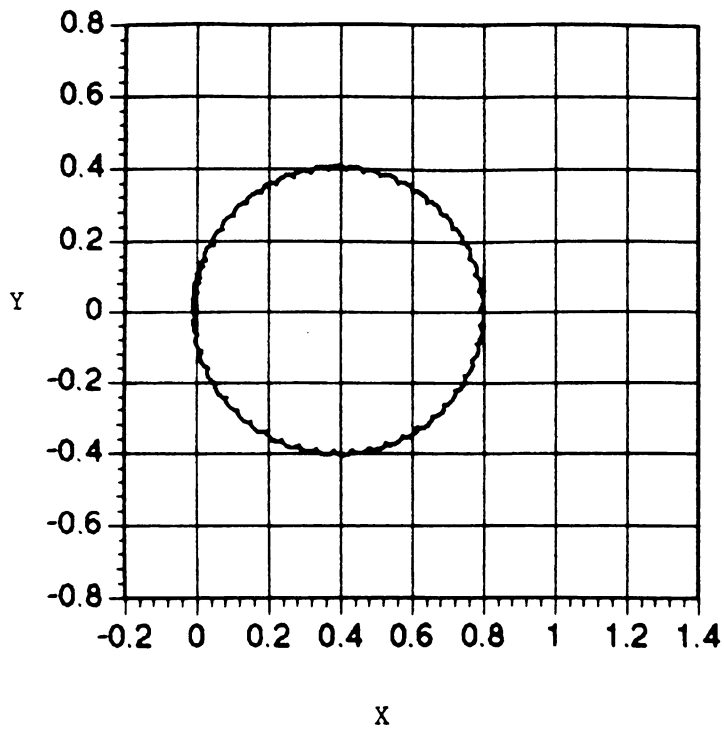

FIG. 5.8

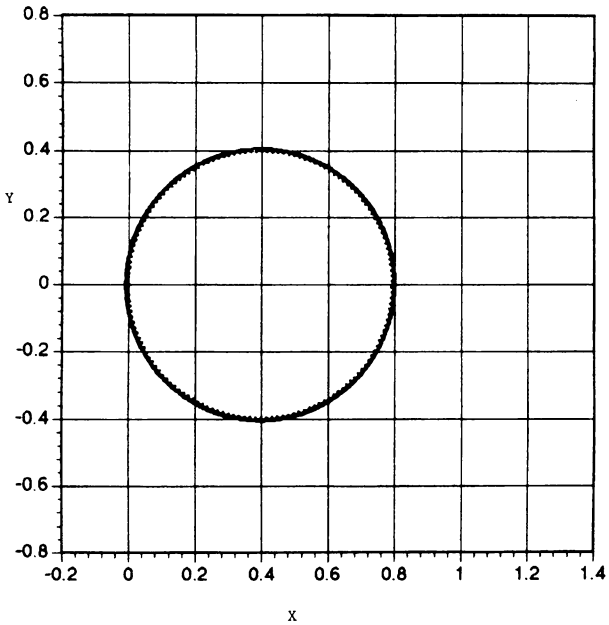

FIG. 5.9

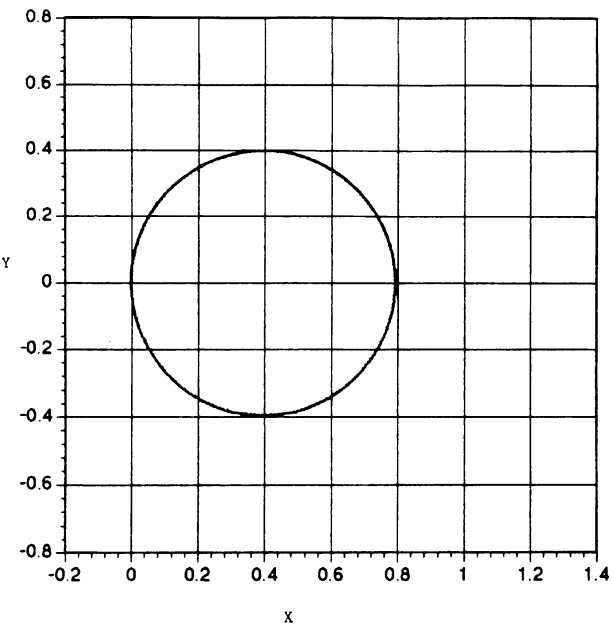

FIG. 5.10

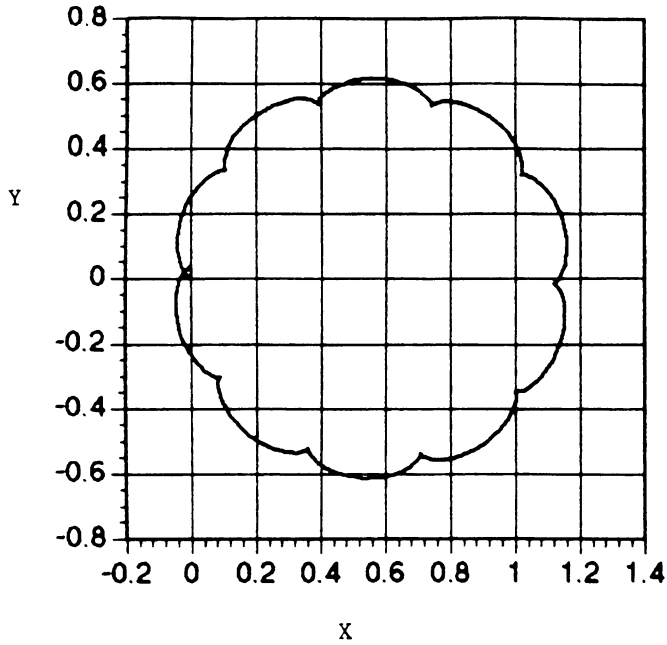

FIG. 5.11

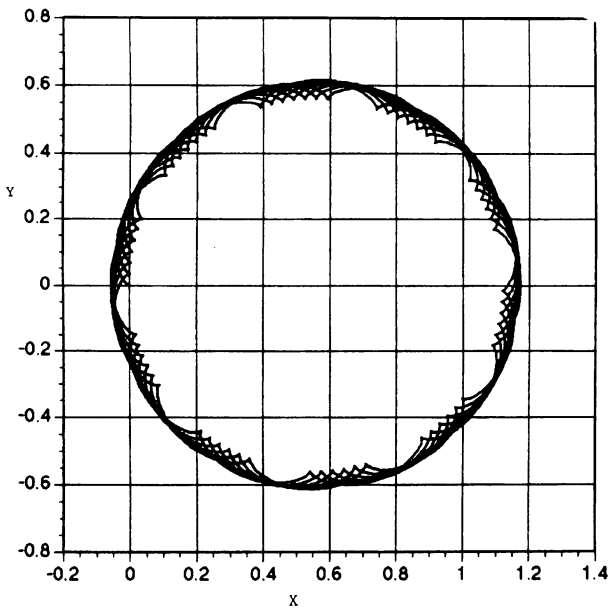

FIG. 5.12

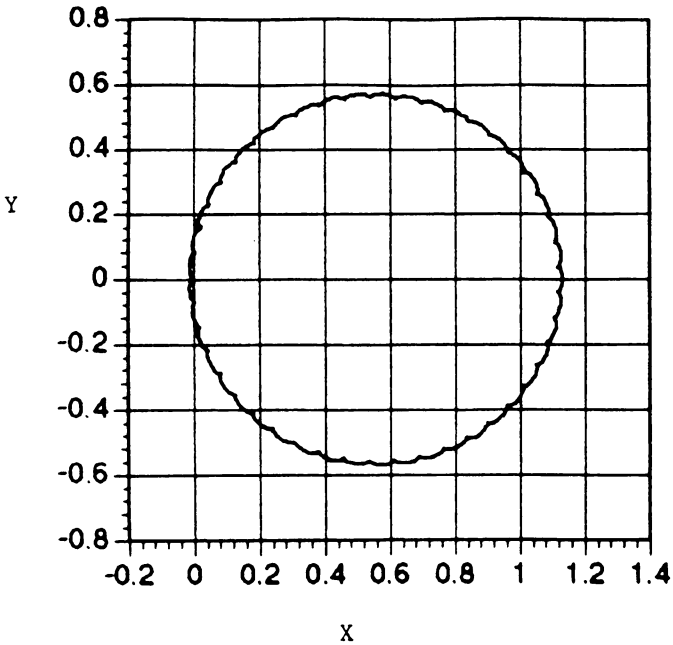

FIG. 5.13

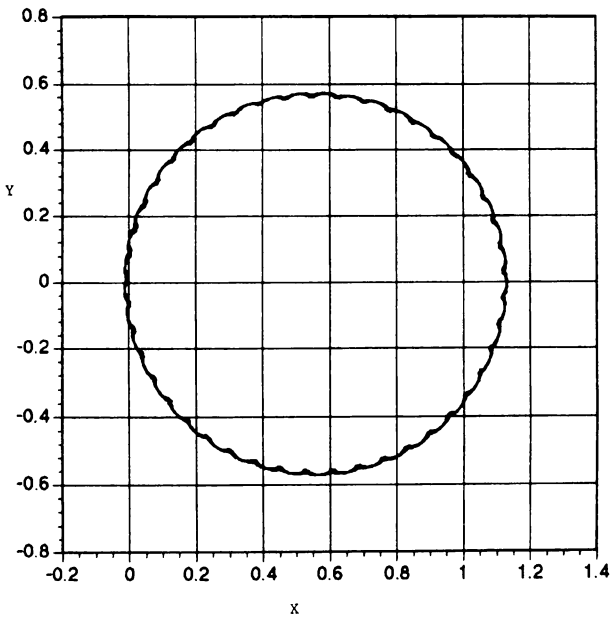

FIG. 5.14

EXAMPLE 9. Set $V = 16, \alpha = 45°$. Figure 5.15 shows the relatively circular trajectory of P_1 in the (X, Y)-plane for all 2200 points, which yields just over 1 cycle. The point $\overline{P}$ is always on the line $(0.5590169945, 0, z)$, with $\overline{z}$ in the range $0.555 < \overline{z} < 0.559$.

EXAMPLE 10. Set $V = 1, \alpha = 15°$. The top falls to the (X, Y)-plane.

Examples 1–9 reveal that each trajectory has a center point, that the trajectories become more circular with increasing V, that the variation in $\overline{z}$ diminishes as V increases, and that the diameter of the trajectory increases with α.

We turn next to the difficult problem [7], [8] of a rotating *nonhomogeneous* top. Note that in earlier sections we used the term *geometric center* throughout rather than *mass center* because of the examples to be considered next.

EXAMPLE 11. Let $V = 4, \alpha = 15°$, as in Example 1, but set $m_2 = 0.995$. The resulting 2200 point trajectory for P_1 in the (X, Y)-plane is shown in Figure 5.16. It shows cusped motion which is similar to that in Figure 5.1 but is in motion to the left. The motion of $\overline{P}$ is fully three dimensional with the projection of its first 100 points shown in Figure 5.17. Although $\overline{y}$ and $\overline{z}$ show only small variations, it is $\overline{x}$ that shows significant motion.

EXAMPLE 12. Let $V = 4, \alpha = 30°$, as in Example 4, but set $m_2 = 1.005$. The results are similar to those in Example 11 and are shown in Figures 5.18 and 5.19. However, this time the motion of P_1 in the (X, Y)-plane is to the right.

EXAMPLE 13. Let $V = 8, \alpha = 30°$, as in Example 5, but set $m_2 = 1.005$ and $m_3 = 0.95$. The entire motion for P_1 is shown in Figure 5.20 and the projection for $\overline{P}$, but for

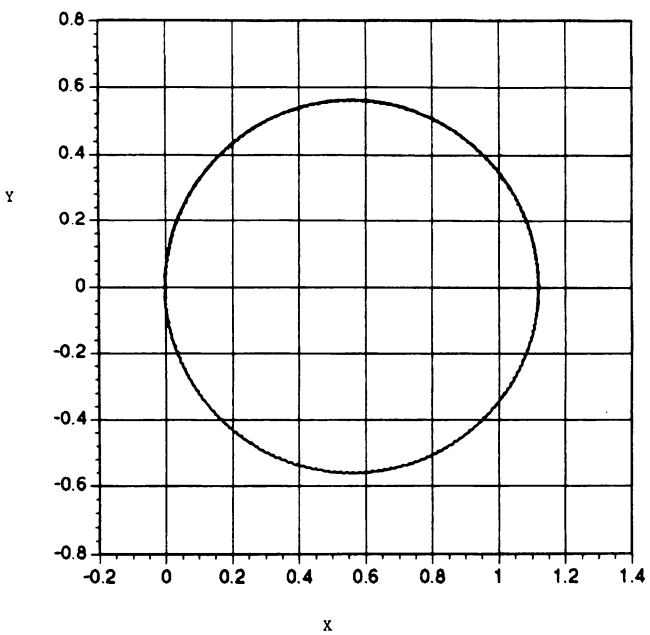

FIG. 5.15

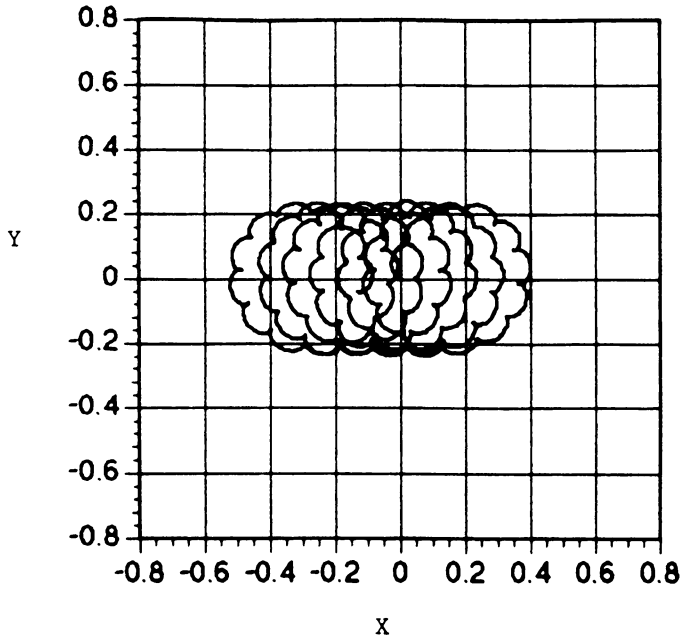

FIG. 5.16

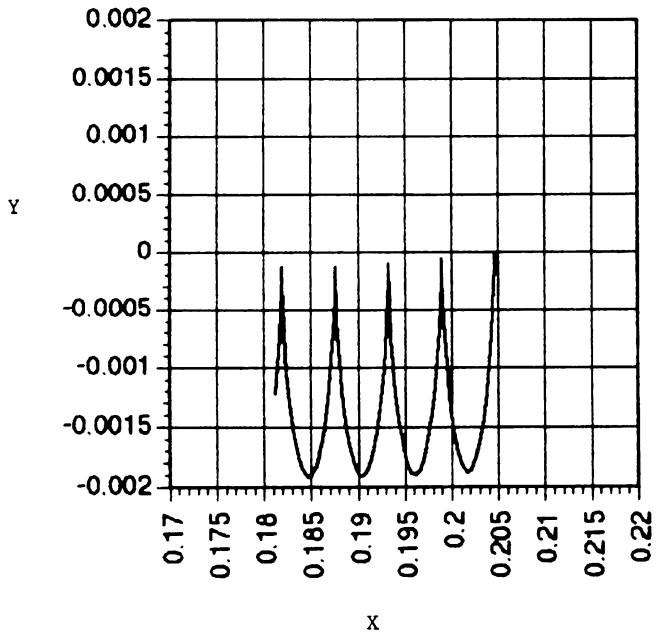

FIG. 5.17

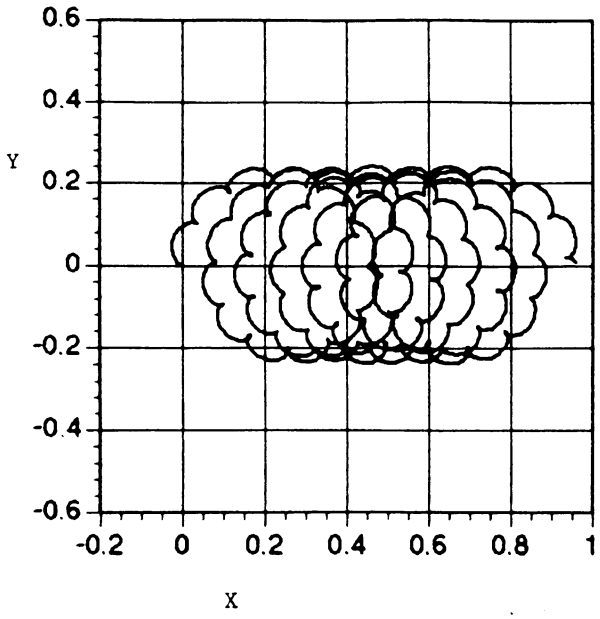

FIG. 5.18

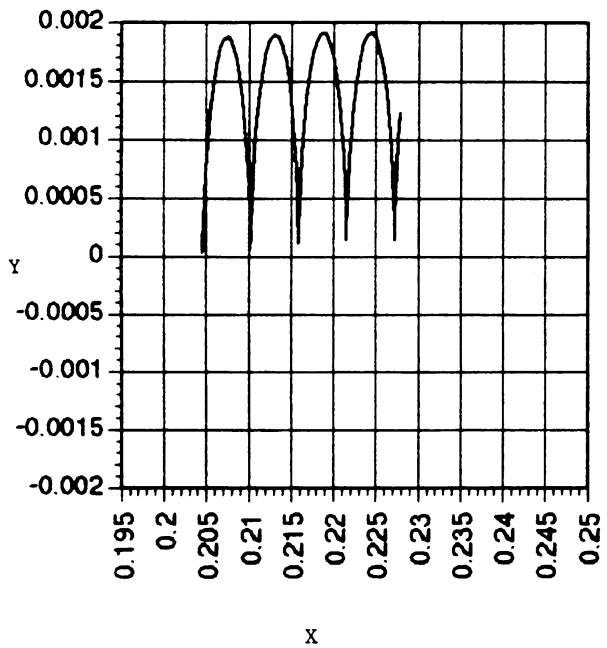

FIG. 5.19

only 100 points, is shown in Figure 5.21. Figure 5.20 shows complex looping motion up and to the right.

EXAMPLE 14. Let $V = 4, \alpha = 45°, m_2 = 0.995, m_3 = 0.985$. The resulting motion of P_1 for the entire 2200 points is shown in Figure 5.22. The projected motion of $\overline{P}$ for the first 100 points is shown in Figure 5.23. The motion of P_1 is up and to the right, but similar to that of Figure 5.18.

With regard to Examples 11–14 and the corresponding graphs in Figures 5.17, 5.19, 5.21, and 5.23, it is worth noting that these graphs, with only 100 points, characterize completely the entire graphs with 2200 points.

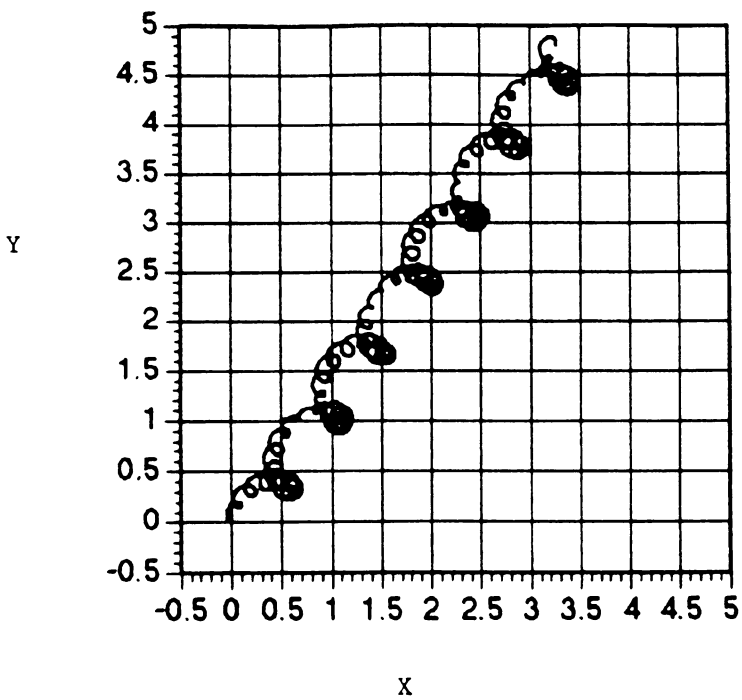

FIG. 5.20

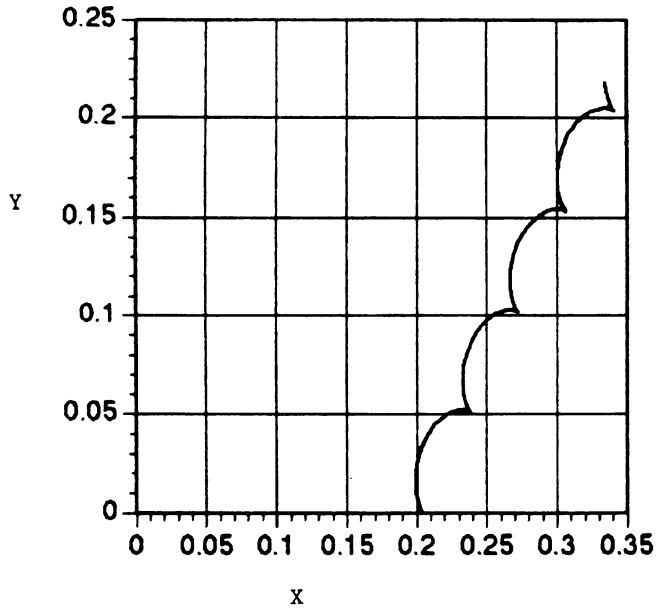

FIG. 5.21

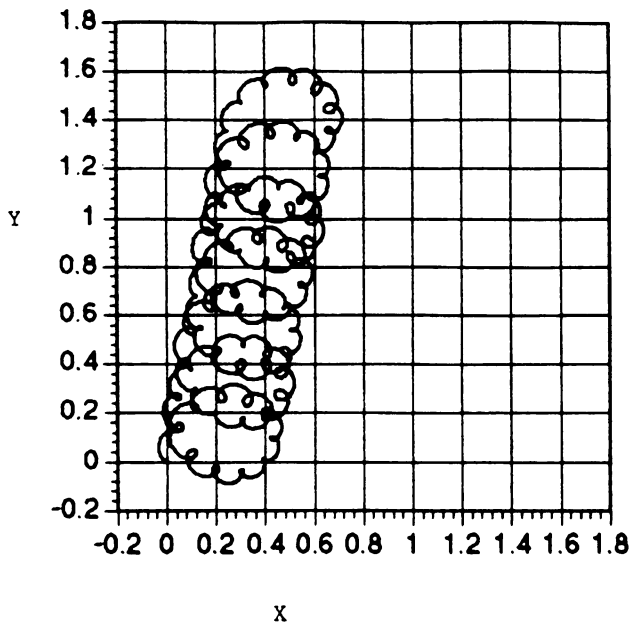

FIG. 5.22

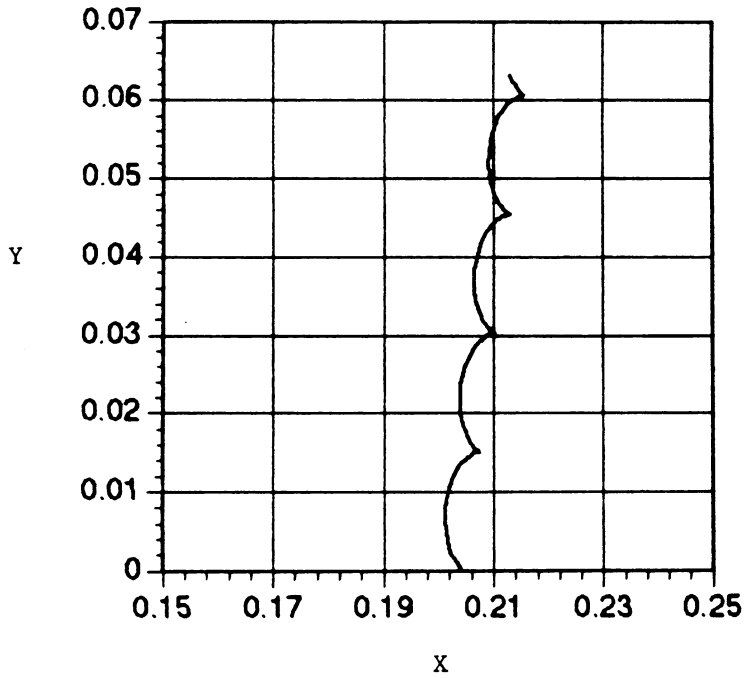

FIG. 5.23

6. Extensions. In order to extend the present discussion to more complex rigid bodies, one can proceed as follows. A given body should be decomposed first into regular tetrahedral building blocks [3], [9]. Let the resulting vertices be $P_1, P_2, \ldots, P_N$. Molecular-type force formulas between pairs of particles can then be applied, but in a fashion so that each particle interacts only with its nearest neighbors. This will preserve rigidity. If a particular material composition is specified, then the total mass need only be distributed equally over $P_1, P_2, \ldots, P_N$. Finally, the resulting N-body problem can be solved in a fashion entirely analogous to that described in Sec. 4.

Note also that any other conservative formula, different from (5.1), which ensures rigidity, may also be used.

REFERENCES

[1] H. Goldstine, *Classical Mechanics*, 2nd Edition, Addison-Wesley, Reading, MA, 1980, Chapters IV, V
[2] R. P. Feynman, R. B. Leighton, and M. Sands, *The Feynman Lectures on Physics*, vol. I, Addison-Wesley, Reading, MA, 1963, Section 20, pp. 5–8
[3] D. Greenspan, *Arithmetic Applied Mathematics*, Pergamon Press, Oxford, 1980
[4] D. Greenspan, *Completely conservative, covariant numerical methodology*, Comput. Math. Applic. **29**, 37–43 (1995)
[5] D. Greenspan, Technical Report #314, Mathematics Dept., UT Arlington, Arlington, TX, 1996
[6] D. Greenspan, *Quasimolecular modelling*, World Sci. Press, Singapore, 1991
[7] A. Gray, *Gyrostatics and Rotational Motion*, Dover, NY, 1959
[8] L. D. Landau and E. M. Lifshitz, *Mechanics* (3rd Edition), Pergamon Press, Oxford, 1976, p. 112
[9] D. Greenspan, *Supercomputer simulation of cracks and fractures by quasimolecular simulation*, J. Phys. Chem. Solids **50**, 1245 (1989)